Electrochemical Oxidation of Nitrite and the Oxidation and Reduction of NO_2 in the Room Temperature Ionic Liquid [C_2mim][NTf_2]

Tessa L. Broder,[†] Debbie S. Silvester,[†] Leigh Aldous,[‡] Christopher Hardacre,[‡] and Richard G. Compton*,[†]

Physical and Theoretical Chemistry Laboratory, University of Oxford, South Parks Road, Oxford OX1 3QZ, United Kingdom, and School of Chemistry and Chemical Engineering/QUILL, Queen's University Belfast, Belfast, Northern Ireland BT9 5AG, United Kingdom

Received: April 11, 2007; In Final Form: May 14, 2007

The electrochemical oxidation of potassium nitrite has been studied in the room temperature ionic liquid (RTIL) [C_2mim][NTf_2] by cyclic voltammetry at platinum electrodes. A chemically irreversible oxidation peak was observed, and a solubility of 7.5(±0.5) mM and diffusion coefficient of 2.0(±0.2) × 10^{-11} m^2 s^{-1} were calculated from potential step chronoamperometry on the microdisk electrode. A second, and sometimes third, oxidation peak was also observed when the anodic limit was extended, and these were provisionally assigned to the oxidation of nitrogen dioxide (NO_2) and nitrate (NO_3^-), respectively. The electrochemical oxidation of nitrogen dioxide gas (NO_2) was also studied by cyclic voltammetry in [C_2mim][NTf_2] on Pt electrodes of various size, giving a solubility of ca. 51(±0.2) mM and diffusion coefficient of 1.6(±0.05) × 10^{-10} m^2 s^{-1} (at 25 °C). It is likely that NO_2 exists predominantly as its dimer, N_2O_4, at room temperature. The oxidation mechanism follows a CE process, which involves the initial dissociation of the dimer to the monomer, followed by a one-electron oxidation. A second, larger oxidation peak was observed at more positive potentials and is thought to be the *direct* oxidation of N_2O_4. In addition to understanding the mechanisms of NO_2^- and NO_2 oxidations, this work has implications in the electrochemical detection of nitrite ions and of NO_2 gas in RTIL media, the latter which may be of particular use in gas sensing.

1. Introduction

Nitrite ions are widely used as an additive in some foods[1] and also as a corrosion inhibitor.[2] The determination of nitrite ions is of huge environmental concern due to the toxicity and potential contribution to environmental release hazards when present in groundwater.[3] As a result, there have been several protocols dealing with the detection of nitrite in water using electrochemical and other methods.[4−6]

The mechanism of nitrite oxidation has been studied in solvents ranging from pure alkali nitrite melts,[7] sodium nitrate−potassium nitrate eutectic melts,[7−11] the aprotic solvent dimethyl sulfoxide (DMSO),[12,13] and water.[14−16] The electro*reduction* of nitrite has also been reported in protic solvents, the mechanism involving participation of water molecules.[3] However, to the best of our knowledge, no obvious reduction peaks have been found in aprotic solvents or melts.

In all media, the *oxidation* of nitrite is thought to proceed by eq 1, resulting in the formation of nitrogen dioxide gas.

$$NO_2^- \rightarrow NO_2(g) + e^- \quad (1)$$

Any further reactions appear to depend on the nature of the solvent. In protic media, NO_2 (or its dimer N_2O_4) is believed to undergo a disproportionation reaction to form nitrate ions (NO_3^-) and protons:[14−16]

$$N_2O_4 + H_2O \rightleftharpoons H^+ + NO_3^- + HNO_2 \quad (2)$$

However, in nitrate melts (KNO_3−$NaNO_3$), the electrogenerated NO_2 reacts with NO_2^- in solution to form nitrate and NO gas:[7,10,11]

$$NO_2 + NO_2^- \rightleftharpoons NO_3^- + NO \quad (3)$$

In DMSO, the mechanism is thought to involve the reaction of NO_2 with NO_2^- to form N_2O_4, followed by association with the solvent.[12,13] In pure molten nitrites, it is believed[7,8] that the only species generated from the oxidation reaction is NO_2, which is in equilibrium with its dimer, N_2O_4. Several reports[7,8,13] have also claimed that the platinum electrode surface (formation of platinum oxides) plays a part in the mechanism. Furthermore, Piela and Wrona[15] claim that the formation of an oxide layer on Pt hinders the nitrite oxidation process in water.

To identify the products following the oxidation of nitrite, it is helpful to study the voltammetry of nitrogen dioxide, NO_2, gas. NO_2 is a brown toxic gas, which causes damage to respiratory organs and contributes to air pollution. The sensing/determination of nitrogen dioxide in air is of huge importance as the gas is emitted from cars, boilers, and other combustion facilities. Several methods have been used to determine NO_2, including those based on electrochemistry.[17,18] Despite the interest in NO_2 detection, there is relatively little reported on the voltammetry and electrochemical mechanism of NO_2 gas dissolved in solvents. Only a few studies[9−11] in KNO_3−$NaNO_3$ melts have reported the addition of NO_2 gas to the solvent, but no voltammetry was shown. However, the electrochemistry of its dimer N_2O_4 (added as a liquid) has been studied in a range

* Author to whom all correspondence should be addressed: E-mail: richard.compton@chemistry.oxford.ac.uk. Phone: +44 (0) 1865-275-413. Fax: +44 (0) 1865-275-410.
[†] University of Oxford.
[‡] Queen's University Belfast.

10.1021/jp0728104 CCC: $37.00
Published on Web 06/16/2007

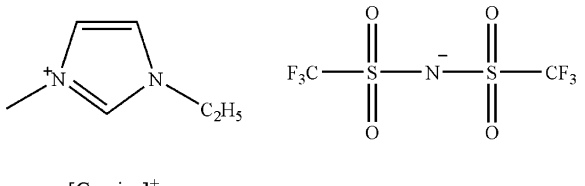

Figure 1. Structures of the anion and cation used as the solvent in this study.

of aprotic solvents by several authors.[19−21] In all cases, a single oxidative wave was reported and is assigned to the following CE mechanism:

$$N_2O_4 \rightleftharpoons 2NO_2 \rightleftharpoons 2NO_2^+ + 2e^- \quad (4)$$

A detailed kinetic study was described in two of these reports,[19,21] but no reductive features were observed. Contrastingly, Boughriet et al.[20] report two reduction steps involving reaction of the dimer with the monomer and suggest that the redox properties are complicated by trace quantities of water, forming N_2O_3, HNO_3, and HNO_2, all electrochemically active species.

The aim of the present study is to explore the oxidation mechanism of nitrite and the redox properties of NO_2 gas in a room temperature ionic liquid (RTIL). RTILs are liquids composed entirely of ions, generally a bulky organic cation and an inorganic anion, and are liquid at and around room temperature. The ability to change the nature of the anion and cation allows for "tuneable" solvents for specific purposes. They possess archetypal properties such as high thermal stability, low volatility, intrinsic conductivity, and wide electrochemical windows, which makes them advantageous particularly for gas sensing[22] and in many other electrochemical applications such as in lithium batteries,[23] capacitors,[24] and solar cells.[25] We have also recently shown that, in the context of nitrate (NO_3^-) oxidation, the ionic liquid solvent (1-ethyl-3-methylimidazolium bis(trifluoromethylsulfonyl)imide $[C_2mim][NTf_2]$) behaved as a "melt" rather than as a conventional aprotic solvent,[26] allowing for the study of nitrate ions at ambient temperatures, and for the formation of an insoluble precipitate of sodium oxide, Na_2O, on the electrode surface, which has shown favorable properties for hydrogen storage.

This work reports the electrooxidation of nitrite ions (from KNO_2) and the oxidation and reduction properties of NO_2 gas dissolved in the RTIL $[C_2mim][NTf_2]$ in order to understand and analyze the reaction mechanisms and kinetics in this media. This work may also have implications in the analytical determination of nitrite ions and in the sensing of nitrogen dioxide gas.

2. Experimental Section

2.1. Chemicals. 1-Ethyl-3-methylimidazolium bis(trifluoromethylsulfonyl)imide ($[C_2mim][NTf_2]$) was prepared in house following standard procedures reported in the literature.[27] Ferrocene (Aldrich, 98%), tetrabutylammonium perchlorate (TBAP, Fluka, Puriss electrochemical grade, >99%), acetonitrile (Fischer Scientific, dried and distilled, >99.99%), potassium nitrite (KNO_2, Aldrich, >96%), nitronium tetrafluoroborate (NO_2BF_4, Aldrich, >95%), cobaltocenium hexafluorophosphate ($Co(C_5H_5)_2PF_6$, Acros Organics, 98%), and NO_2 gas (Argo International, 99.5%) were used as received, without further purification.

2.2. Instrumentation. *2.2.1. Preparation of Solutions.* A saturated solution of KNO_2 was prepared by dissolving approximately 2 mg of solid in 1 mL of $[C_2mim][NTf_2]$. The solution was stirred overnight to allow for full dissolution. A 30 mM solution of NO_2BF_4 was prepared by dissolving 10 mg of the solid in 2 mL of $[C_2mim][NTf_2]$ (dried under vacuum at 0.05 Torr for 24 h at 80 °C).

2.2.2. Electrochemical Experiments. Cyclic voltammetry was performed using a computer-controlled μ-Autolab potentiostat (Eco-Chemie, Netherlands). For experiments involving KNO_2, a conventional two-electrode arrangement was employed, with a platinum electrode (10 μm diameter) as the working electrode. A 0.5 mm diameter silver wire was used as a quasireference electrode. The electrodes were housed in a glass "T-cell"[28,29] specifically designed for examining microsamples of RTILs under a controlled atmosphere. The microelectrode was modified with a section of disposable micropipet tip, creating a small cavity above the disk into which 20 μL of the KNO_2 stock solution (described above) was placed. Experiments for KNO_2 and NO_2BF_4 with 100 μm or 0.5 mm diameter platinum working electrodes were carried out using a three-electrode arrangement in a small cell (described elsewhere),[30] with a 0.5 mm diameter silver wire as a quasireference electrode and a platinum coil as a counter electrode. The cell was kept under a constant flow of nitrogen throughout measurements.

Experiments involving NO_2 gas on a 10 μm Pt working electrode were performed in the "T-cell"[28,29] (described above), with 20 μL of "blank" ionic liquid in the cavity above the electrode. A PTFE tube leading directly from the NO_2 gas cylinder was attached to one arm of the cell, and an outlet PTFE tube to the other. The gas (brown in color) was allowed to diffuse through the cell, passing over the solution, until equilibrium was achieved (typically after 20 min, as evidenced by maximum stable peak currents). The solution turned dark green after approximately 2 min. For experiments involving NO_2 on the 100 μm and 0.5 mm diameter Pt working electrodes, a sealed five-necked flask was used. A 0.5 mm diameter silver wire was employed as a quasireference electrode and a 0.5 mm diameter platinum wire as a counter electrode. A 1 mL sample of "blank" RTIL was placed under vacuum for 2 h and then transferred to the five-necked flask. Two large syringe needles were attached to the inlet and outlet PTFE tubing and used to pierce the seals of two necks of the flask. This allowed a constant flow of NO_2 gas over the RTIL throughout the experiments. The three other necks of the flask were used to house the electrodes. The solution showed a light green color after approximately 10 min. All experiments involving NO_2 were performed in a fume cupboard.

The microelectrode was polished on soft lapping pads (Kemet Ltd., UK) using 1.0 μm and 0.3 μm aqueous-alumina slurries (Buehler, Illinois). The microdisk radius was calibrated electrochemically by analyzing the steady-state voltammetry of a 2 mM solution of ferrocene in acetonitrile, containing 0.1 M TBAP as a supporting electrolyte, using a value for the diffusion coefficient of 2.3×10^{-9} m^2 s^{-1} at 298 K.[31]

2.3. Chronoamperometric Experiments. Chronoamperometric transients were achieved with use of a sample time of 0.1 s. The potential was held at 0 V for 20 s for pretreatment, after which the potential was stepped to the required value and the current was measured for 10 s. Fitting of the experimental data was achieved by using the nonlinear curve fitting function available in Origin 7.0 (MicroCal Software Inc.), following the Shoup and Szabo[32] approximation, as employed by Evans et al.[33] The equations used in this approximation are sufficient to

describe the current response to within an accuracy of 0.6%, and are given below

$$I = -4nFDcr_d f(\tau) \quad (5)$$

$$f(\tau) = 0.7854 + 0.8863\tau^{-1/2} + 0.2146e^{-0.7823x^{-1/2}} \quad (6)$$

$$\tau = \frac{4Dt}{r_d^2} \quad (7)$$

where n is the number of electrons transferred, F is the Faraday constant, D is the diffusion coefficient, c is the initial concentration of parent species, r_d is the radius of the microdisk, and t is the time. The software was instructed to perform 100 iterations on the data, fixing the value for the electrode radius, which was previously calibrated. When the experimental data had been optimized, a value for the diffusion coefficient and the product of the number of electrons multiplied by the concentration was obtained.

3. Results and Discussion

The RTIL chosen as the solvent in this study was $[C_2mim][NTf_2]$ due to its wide electrochemical window, clean baseline, and relatively low viscosity (28 cP),[34] which gives higher current responses at microelectrodes. All results below are reported in this medium.

3.1. The Oxidation of Potassium Nitrite (KNO_2) in $[C_2mim][NTf_2]$. Figure 2a shows the oxidation of a saturated solution of KNO_2 in $[C_2mim][NTf_2]$ on a Pt microelectrode (diameter 10 μm) at a range of scan rates from 10 mV s^{-1} to 1 V s^{-1}. A single oxidative peak is observed in the voltage range from +0.4 to +1.3 V vs Ag, which is assigned to the following reaction:

$$NO_2^- \rightarrow NO_2(g) + e^- \quad (1)$$

This is directly comparable to oxidation peaks observed in protic media,[14−16] in DMSO,[12,13] in KNO_3-NaNO_3 melts,[7,9,10,35] and in pure nitrite melts.[7] The oxidation peak shown in Figure 2a becomes more transient shaped at higher scan rates, and a plot of peak current vs square root of the scan rate is linear, indicating that the process is diffusion controlled. The peak also appears chemically irreversible, as shown by the absence of any back peak following the oxidation at all scan rates studied.

Several authors[10,11,35] have suggested that the oxidation reaction (eq 1) is chemically reversible, whereas others have shown its irreversibility.[12−15] To understand this discrepancy, Desimoni et al.[35] showed that the oxidation peak of nitrite was chemically reversible in KNO_3-NaNO_3 melts, but became more irreversible with the addition of small amounts of water. The overall catalytic mechanism shown in eq 8 was thought to be in competition with the simple electrode process given in eq 1.[35]

$$NO_2^- + H_2O \rightleftharpoons NO_3^- + 2H^+ + 2e^- \quad (8)$$

To confirm the irreversibility of the oxidation in $[C_2mim][NTf_2]$, the same saturated solution of KNO_2 was studied on a larger Pt disk electrode, demonstrating slower apparent electrode kinetics. Figure 2b shows cyclic voltammograms for the oxidation of a saturated solution of KNO_2 on a Pt electrode (diameter 0.5 mm) at scan rates of 10 mV s^{-1} to 1 V s^{-1}. Again, a single oxidative peak is observed that shows no reduction peaks at all scan rates studied, even when the reverse scan was swept to −2.0 V (not shown here). This suggests that reaction 1 is chemically irreversible in RTIL media, possibly due to reaction with trace water present in the ionic liquid, following eq 8. We note here that no obvious voltammetry from water was observed when the ionic liquid was further dried under vacuum for 2 h, suggesting that the amount of water present may be in a small enough quantity not to be detected voltammetrically.

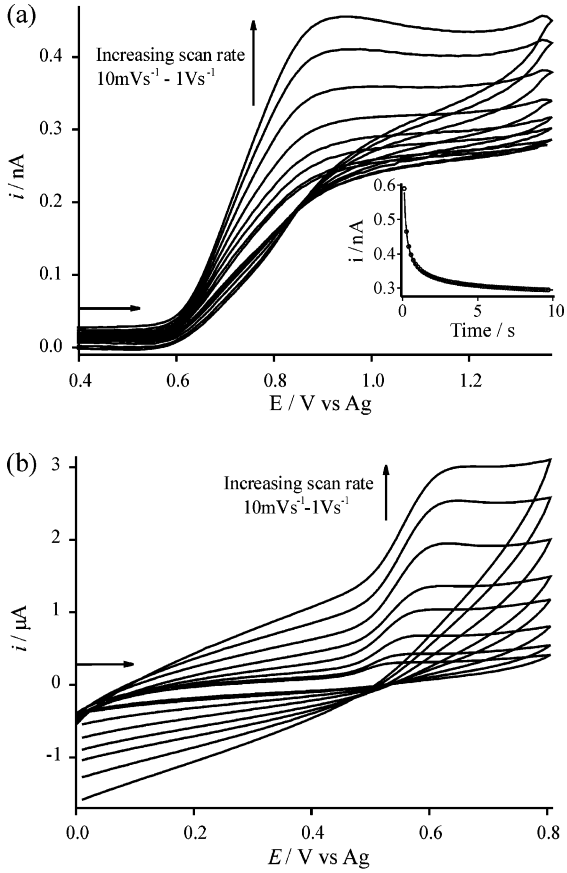

Figure 2. Cyclic voltammograms for the oxidation of a saturated solution of KNO_2 in $[C_2mim][NTf_2]$ on (a) a Pt microelectrode (d = 10 μm) and (b) a Pt macroelectrode (d = 0.5 mm) at scan rates of 10, 20, 50, 100, 200, 400, 700, and 1000 mV s^{-1}. The inset to panel a shows the experimental (—) and fitted theoretical (●) chronoamperometric transients for the oxidation of KNO_2 in $[C_2mim][NTf_2]$ on a 10 μm diameter Pt electrode. The potential was stepped from +0.4 to +1.2 V.

To calculate a concentration (solubility) and diffusion coefficient of KNO_2 in $[C_2mim][NTf_2]$, a potential step was performed on the oxidative wave. The potential was stepped from +0.4 to +1.2 V on a 10 μm diameter Pt electrode, and the current was measured for 10 s. The inset to Figure 2a shows the experimental (solid line) and theoretically fitted (dots) chronoamperometric transients. The experimental data were fitted to the Shoup and Szabo[32] expression, and gave a concentration (solubility) of 7.5(±0.5) mM and a diffusion coefficient of 2.0(±0.2) × 10^{-11} m^2 s^{-1}, which is approximately 2 orders of magnitude less than that in water (1.8 × 10^{-9} m^2 s^{-1}),[36] and is reasonable given the higher viscosity of the RTIL (28 cP)[34] compared to water (1 cP). The modest solubility is also consistent with that observed previously for $NaNO_3$ and KNO_3 in the same RTIL.[26]

On sweeping the potential more positive, a further oxidative wave was observed, and the voltammetry is shown in Figure 1 in the Supporting Information. On the 10 μm Pt microelectrode, there was also evidence of a third oxidation peak (not shown

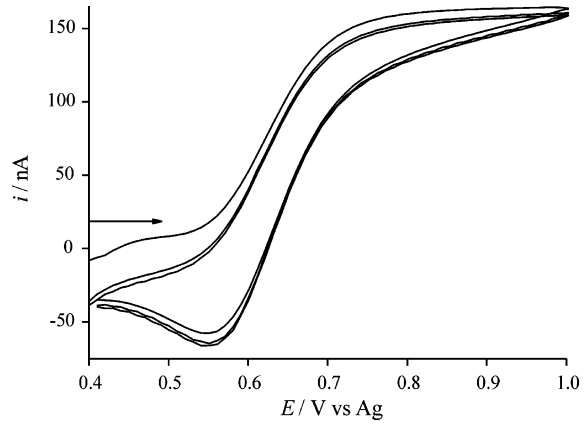

Figure 3. Cyclic voltammograms (three repeat scans) for the oxidation of NO_2 gas in [C_2mim][NTf_2] on a Pt microelectrode ($d = 10$ μm) at a scan rate of 1 V s^{-1}.

here), but this was very broad and undefined, and only observed intermittently.

To suggest the identity of the three oxidation peaks, the voltammetry of nitrite was referenced to the ferrocene/ferrocenium (Fc/Fc^+) redox couple in solution. As the peak potentials of nitrite oxidation and Fc/Fc^+ are similar, the voltammetry of nitrite was first referenced to cobaltocenium/cobaltocene (Cc^+/Cc), and then adjusted to Fc/Fc^+. Ferrocene is recommended by IUPAC[37] as a stable redox couple in aprotic media, and has been used in RTILs for this purpose.[38] The oxidation of ferrocene occurred at a potential of +0.85 V in this solution, which gives the positions of the three oxidation peaks as ca. +0.20, +1.13, and + 1.57 V vs Fc. The identity of the second peak is thus provisionally thought to be the oxidation of NO_2 (monomer), which was formed in eq 1, as the peak potential is similar to that of NO_2 oxidation (+1.10V vs Fc, see section 3.2). This suggests that if eq 8 is occurring, it is either not instantaneous or does not go to completion in this medium. The third peak is likely the oxidation of NO_3^- (produced in eq 8), as the peak potential matches that of NO_3^- vs ferrocene (not shown here).

3.2. The Oxidation of NO_2 Gas in [C_2mim][NTf_2]. To explore the oxidation/reduction mechanisms and kinetics of NO_2, and to show the possible analytical utility of RTILs as a gas sensor for NO_2, the voltammetry of NO_2 was obtained on three Pt electrodes of diameter 10 μm, 100 μm, and 0.5 mm. Figure 3 shows the oxidation of NO_2 gas (100%) in [C_2mim][NTf_2] on a 10 μm diameter Pt electrode in the potential range +0.4 to +1.0 V. Three repeat cycles are overlaid at a scan rate of 1 V s^{-1}. A steady-state oxidation peak at ca. +0.86 V (vs Ag) is observed, with a corresponding transient-shaped reduction peak at +0.55 V, which is stable on successive cycles. The oxidation peak current is relatively high compared to that of KNO_2 (Figure 2a), suggesting a larger solubility of NO_2 in [C_2mim][NTf_2] (solubility values discussed below).

The experiments were then repeated under the same conditions on two larger Pt electrodes of diameter 100 μm and 0.5 mm, and are shown in panels a and b of Figure 4, respectively, at a range of scan rates. A plot of peak current vs square root scan rate for the oxidation peak on the 100 μm diameter Pt electrode (Figure 4a) is linear, indicating that the process is diffusion controlled. However, the same plot on the larger (0.5 mm diameter) Pt electrode is curved, suggesting that the process may be controlled by a chemical step preceding the electrochemical step. This suggests that NO_2 probably exists in solution as its more stable dimer, N_2O_4, and undergoes dissociation

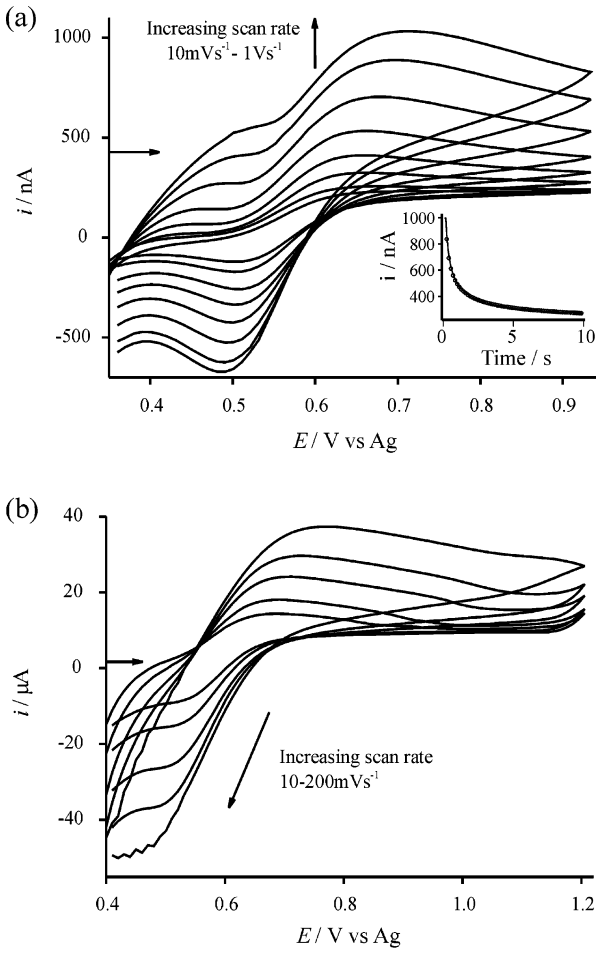

Figure 4. Cyclic voltammograms for the oxidation of NO_2 gas in [C_2-mim][NTf_2] on (a) a Pt microelectrode ($d = 100$ μm) at scan rates of 10, 20, 50, 100, 200, 400, 700, and 1000 mV s^{-1} and (b) a Pt macroelectrode ($d = 0.5$ mm) at scan rates of 10, 20, 50, 100, and 200 mV s^{-1}. The inset to panel a shows the experimental (—) and fitted theoretical (●) chronoamperometric transients for the oxidation of NO_2 on a 100 μm diameter Pt electrode. The potential was stepped from +0.4 to +0.9 V.

before the electrochemical step. This is in agreement with that observed by Amatore et al.[21] and Wartel et al.,[19,20] who propose the following CE mechanism:

$$N_2O_4 \underset{k_{-1}}{\overset{k_1}{\rightleftharpoons}} 2NO_2 \quad (9)$$

$$NO_2 \xrightarrow{k_s} NO_2^+ + e^- \quad (10)$$

There was also no voltammetric evidence to suggest that heterolytic dissociation occurs in this medium. It is believed that the corresponding reduction peak in Figures 3 and 4 is thus due to the reduction of the nitronium cation, NO_2^+, back to NO_2. This was further confirmed separately by matching the peak positions of NO_2^+/NO_2 vs ferrocene (not shown here), using nitronium tetrafluoroborate, [NO_2][BF_4], as the source of the nitronium cation. We note here that the addition of NO_2 gas shifted the peak potential of ferrocene oxidation very significantly, and that the positions (at 100 mV s^{-1}) of the oxidative and reductive waves on the 10 μm diameter Pt electrode are +1.10 and +0.84 V vs Fc oxidation respectively. The above mechanism is then used to simulate the oxidative peak of NO_2 on a 0.5 mm diameter Pt electrode in the one-dimensional simulation program DigiSim 3.03 (BAS Technicol)[39] and is discussed later in Section 3.2.1.

TABLE 1: Parameters Employed in the Simulation of NO_2 Oxidation (First Wave) Following Eqs 9 and 10 at 25 °C

$[N_2O_4] = 46(\pm 5)$ mM	$K = 6.0(\pm 0.5) \times 10^{-4}$ mol dm^{-3}
$[NO_2] = 140(\pm 10)$ mM	$k_1 = 10(\pm 0.5)$ s^{-1}
area of disk $= 1.96 \times 10^{-3}$ cm^2	$k_{-1} = 1.67(\pm 0.2) \times 10^4$ dm^3 mol^{-1} s^{-1}
$E_0 = 0.50$ V	$D_{N_2O_4} = 1.5(\pm 0.1) \times 10^{-6}$ cm^2 s^{-1}
$\alpha = 0.5$	$D_{NO_2} = 5.0(\pm 0.4) \times 10^{-6}$ cm^2 s^{-1}
$k_s = 0.002(\pm 0.0001)$ cm s^{-1}	$D_{NO_2^+} = 6.0(\pm 0.5) \times 10^{-6}$ cm^2 s^{-1}

To calculate the solubility of NO_2 (or N_2O_4) in $[C_2mim][NTf_2]$, a potential step was performed on the oxidative wave of NO_2. The potential was stepped from +0.4 to +0.9 V on the 100 μm diameter Pt electrode (which gave a better fit (ca. ±0.7% for both D and nc) to the Shoup and Szabo[32] expression than on the 10 μm diameter Pt electrode) and the current was measured for 10 s. The resulting chronoamperometric transient is shown as a solid line (Figure 4a inset), together with the theoretical fit (dots). The solubility of NO_2 in $[C_2mim][NTf_2]$ was calculated to be 51.2(±0.2) mM, which is more than 10 times greater than that observed in KNO_3-NaNO_3 melts (5 mM at 300 °C[10] and 2 mM at 250 °C),[11] suggesting the possibility of using RTILs as NO_2 potential gas sensing media. The diffusion coefficient of NO_2 (D_{NO_2}) in $[C_2mim][NTf_2]$ was found to be $1.59(\pm 0.05) \times 10^{-10}$ m^2 s^{-1}, which is of the same order of magnitude as O_2 in $[C_2mim][NTf_2]$ (8.3×10^{-10} m^2 s^{-1}),[40] and ca. 1 order of magnitude less than D_{NO_2} in the aprotic solvents dichloromethane (DCM), nitromethane (NM), acetonitrile (MeCN), and propylene carbonate (PC) (1.4,[21] 1.1,[19] 1.8,[21] and $0.28^{19} \times 10^{-9}$ m^2 s^{-1}, respectively), which is reasonable given the higher viscosity of the RTIL (28 cP) compared to DCM (0.44 cP), NM (0.61 cP), MeCN (0.34 cP), and PC (2.5 cP).

3.2.1. Simulating the Oxidation of NO_2 Gas in $[C_2mim][NTf_2]$ on a 0.5 mm Diameter Pt Electrode. The one-dimensional simulation program DigiSim 3.03 (BAS Technicol)[39] was used to model the oxidative wave of NO_2 on a 0.5 mm diameter Pt electrode at a range of scan rates. The generic reaction scheme used in the simulation was:

$$A = 2B \tag{11}$$

$$C + e^- = B \tag{12}$$

where $A = N_2O_4$, $B = NO_2$, and $C = NO_2^+$. It was found that the oxidative wave could be best simulated under a set of kinetic parameters, given in Table 1. The diffusion coefficient of N_2O_4 was 1.5×10^{-6} cm^2 s^{-1}, very similar to that obtained from chronoamperometry (see above), and the diffusion coefficients of NO_2 and NO_2^+ were adjusted accordingly to give the best fit. The initial concentration of N_2O_4 was varied close to the value of 51 mM (from chronoamperometry), with the best fit obtained when the concentration was 46(±0.5) mM. The remaining kinetic parameters (electrochemical rate constant, k_s, homogeneous equilibrium constant, K, rate constants for the forward and backward reactions, k_1 and k_{-1}) were then also iterated to give the best possible fit, and are given in Table 1. The experimental (solid line) and simulated voltammograms (dots) for the oxidation of NO_2 on a 0.5 mm diameter Pt electrode are shown in Figure 5 at scan rates of (a) 20, (b) 50, (c) 100, and (d) 200 mV s^{-1}. These figures represent the best fit obtained from simulation of the mechanism given by eqs 11 and 12.

It was found that the parameters given in Table 1 are comparable to those obtained in dichloromethane (DCM).[21] In DCM, k_s, K, k_1, and k_{-1} were found to be 0.017 cm s^{-1}, 6.0×10^{-4} mol dm^{-3}, 10 s^{-1}, and 1.8×10^4 dm^3 mol^{-1} s^{-1}, respectively.[21] In the RTIL $[C_2mim][NTf_2]$, these numbers are almost exactly the same, with the exception of k_s, which is 0.002 cm s^{-1} in the RTIL, indicating slower kinetics for the electrochemical step. This is not unexpected in a qualitatively different medium (28 cP compared to 0.44 cP) and also given the smaller electrode size used here in the RTIL study (0.5 mm diameter compared to 1 mm diameter in DCM).[21] These results suggest that the same mechanism for the oxidation of NO_2 (N_2O_4) is taking place inside an RTIL as in conventional solvents such as dichloromethane,[21] nitromethane,[19] acetonitrile,[21] and propylene carbonate.[19]

3.2.2. Extension of the Anodic Window. Unlike previous studies for the oxidation of NO_2,[19-21] a second oxidative wave was observed when the anodic window was extended further. This is a result of the wider accessible electrochemical window available in RTILs compared to conventional solvents. Figure 6 shows the oxidation of NO_2 (or its dimer N_2O_4) in $[C_2mim][NTf_2]$ on (a) a 100 μm diameter Pt electrode and (b) on a 0.5 mm diameter Pt electrode, at a range of scan rates. The second oxidation appeared outside the accessible solvent window on the 10 μm diameter electrode, and hence is not shown. The first oxidation peak shown in Figure 4a (100 μm diameter electrode) is present at ca. +0.7 V vs Ag (+1.10 V vs Fc), and there is a second, much larger oxidative peak at +1.89 V (+2.24 V vs Fc, at 100 mV s^{-1}). This second oxidation is also observed at +1.54 V (+1.89 V vs Fc, 100 mV s^{-1}) on the 0.5 mm diameter electrode. In both cases, the separation between the second oxidation peak and the reduction peak increases with scan rate (more dramatically on the larger 0.5 mm diameter Pt electrode), indicating that the system is not fully reversible, and complicated by follow-up chemistry in the mechanism. Furthermore, attempts to fit a potential step (chronoamperometric transient) to the Shoup and Szabo[32] expression were unsuccessful for the second wave, supporting this conclusion. In light of these findings, we tentatively suggest that the second oxidation wave corresponds to the direct oxidation of N_2O_4, possibly following an ECE mechanism given below:

$$N_2O_4 \rightarrow N_2O_4^+ + e^- \tag{13}$$

$$N_2O_4^+ \rightleftharpoons NO_2 + NO_2^+ \tag{14}$$

$$NO_2 \xrightarrow{k_s} NO_2^+ + e^- \tag{10}$$

This mechanism is further supported by the observation that the reduction peak at ca. +0.4 V (reduction of the nitronium cation) gets larger on repeat cycles, indicating that the nitronium cation (NO_2^+) is a product of the second oxidation. To demonstrate this, Figure 7 shows five consecutive cyclic voltammograms for the oxidation of NO_2 in $[C_2mim][NTf_2]$ on a 0.5 mm diameter Pt electrode at a scan rate of 1 V s^{-1}. The peak current of the reduction peak at ca. +0.4 V vs Ag increases systematically on consecutive cycles, despite the fact that the second oxidation peak at ca. +1.89 V decreases. This evidence allows the suggestion of the identity of the second peak to be the direct oxidation of N_2O_4, which is not unreasonable given the higher potentials required for direct oxidation.

3.3. The Reduction of NO_2 Gas in $[C_2mim][NTf_2]$. As a final step in investigating the full electrochemical mechanism of NO_2 in $[C_2mim][NTf_2]$, the reductive window was next studied. Figure 8a shows the reduction of NO_2 starting at +1.25 V in $[C_2mim][NTf_2]$ on a 0.5 mm diameter Pt electrode at a scan rate of 100 mV s^{-1}. In starting at a positive potential, the initial reduction peak as seen in Figure 4b (part of the redox

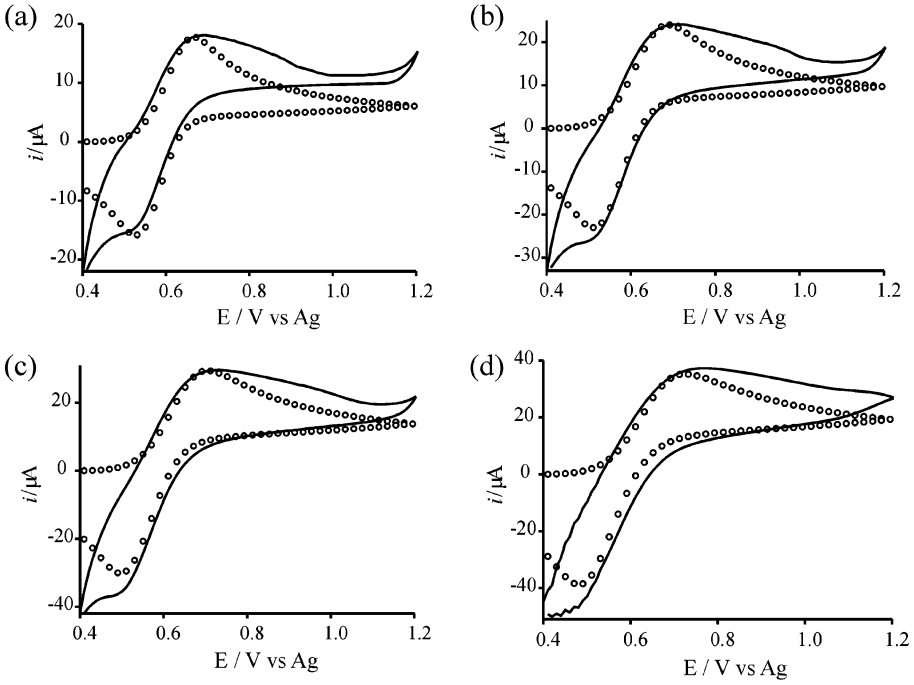

Figure 5. A comparison of experimental (—) and simulated (○) cyclic voltammetry for the oxidation of NO_2 in [C_2mim][NTf_2] on a Pt macroelectrode (d = 0.5 mm) at scan rates of (a) 20, (b) 50, (c) 100, and (d) 200 mV s^{-1}.

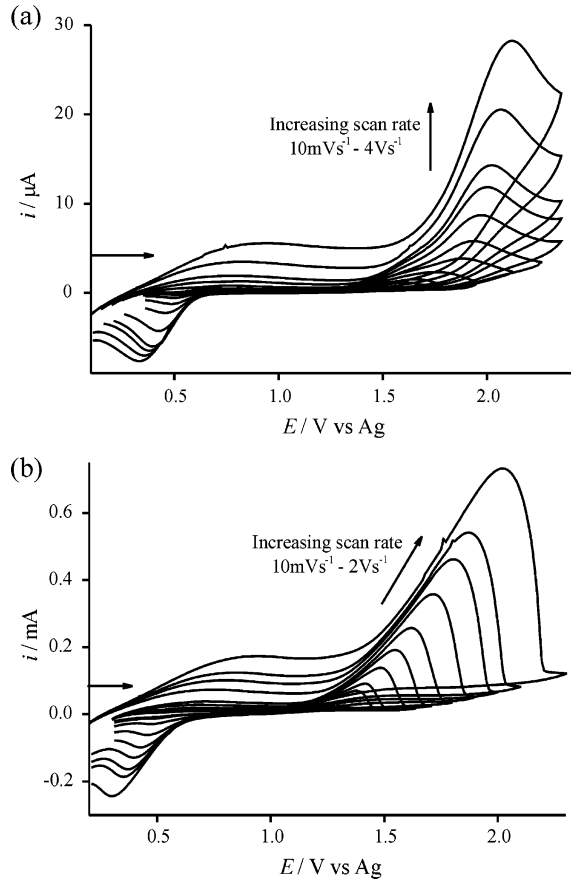

Figure 6. Cyclic voltammetry for the oxidation of NO_2 gas in [C_2mim][NTf_2] with an extended anodic window on (a) a Pt microelectrode (d = 100 μm) at scan rates from 10 to 4000 mV s^{-1} and (b) a Pt macroelectrode (d = 0.5 mm) at scan rates from 10 to 2000 mV s^{-1}.

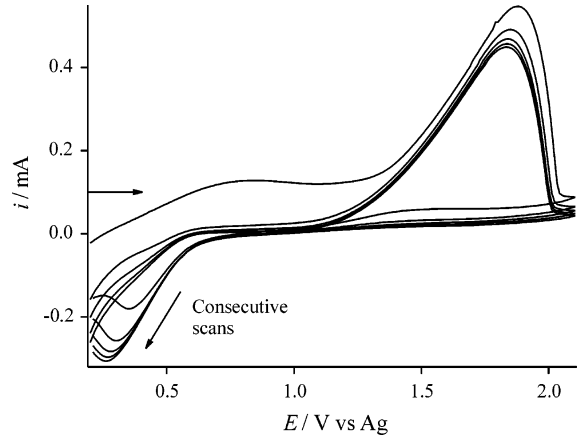

Figure 7. Cyclic voltammetry for the oxidation of NO_2 gas in [C_2mim][NTf_2] with an extended anodic window on a Pt macroelectrode (d = 0.5 mm). Five consecutive scans are shown at a scan rate of 1 V s^{-1}.

couple given in eqs 8 and 9) at ca. +0.5 V is clearly evident. At more negative potentials, there is a much larger reduction peak (at −0.62 V, −0.11 V vs Fc), with a corresponding broad oxidative wave (at +0.49 V vs Ag, +1.0 V vs Fc). The peak separation is much too large to be from oxygen (cf. $\Delta E(O_2/O_2^{\bullet-})$ = 0.35 V in [C_2mim][NTf_2])[40] and therefore must be due to the reduction of NO_2 (N_2O_4) in solution. Figure 8b shows cyclic voltammograms for the reduction of NO_2 in [C_2mim][NTf_2] on a Pt electrode (diameter 0.5 mm) at scan rates from 10 to 200 mV s^{-1}. A plot of peak current vs square root scan rate for the reductive wave was linear, indicating that the process is diffusion controlled. The peak separations increase dramatically with scan rate, suggesting that the process is strongly electrochemically irreversible.

There are very few literature reports showing the reduction of NO_2; however, Boughriet et al.[20] state that two reductive waves were observed following the reduction of N_2O_4 in sulfanone. They propose that the first wave corresponds to the reduction:

$$NO_2 + N_2O_4 + e^- \rightleftharpoons N_2O_3 + NO_3^- \qquad (15)$$

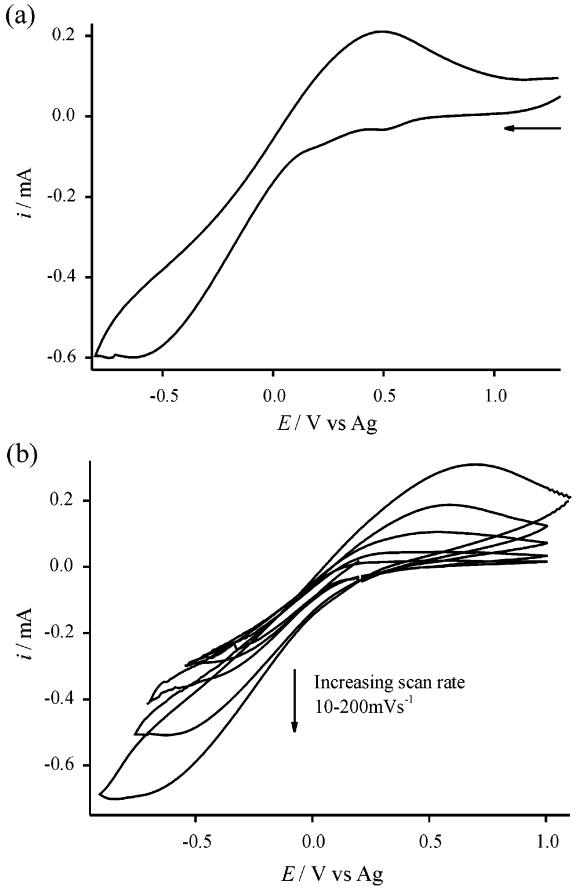

Figure 8. Cyclic voltammograms for the reduction of NO_2 gas in the RTIL $[C_2mim][NTf_2]$ on a Pt macroelectrode ($d = 0.5$ mm) starting from (a) +1.25 (scan rate 100 mV s^{-1}) and (b) +0.2 V (scan rates of 10, 20, 50, 100, and 200 mV s^{-1}).

and the second wave corresponds to either/all of the following equations:

$$3N_2O_4 + 2e^- \rightleftharpoons 2N_2O_3 + 2NO_3^- \quad (16)$$

$$N_2O_4 + e^- \rightleftharpoons NO + NO_3^- \quad (17)$$

$$2N_2O_3 + e^- \rightleftharpoons 3NO + NO_3^- \quad (18)$$

It is likely that some or all of these processes operate in the RTIL medium. Furthermore, successful fitting to a chronoamperometric transient was not achieved, suggesting that the reduction is not a simple *n*-electron-transfer step, which is consistent with the above equations. It is difficult to determine the nature of any intermediates, although there was no evidence of any deposit on the electrode surface following the reduction. We note here that two isomers of N_2O_4 are possible (O_2N-NO_2 and $ONO-NO_2$), which would be likely to exhibit different redox behavior, although we have seen no voltammetric evidence to distinguish between the two. Since the peaks are relatively broad, it may be possible that they both exist and contribute to the peak shape in Figure 8.

4. Conclusions

The electrochemical oxidations of the nitrite ion (from KNO_2) and nitrogen dioxide gas (NO_2) in $[C_2mim][NTf_2]$ have been studied by cyclic voltammetry on various Pt electrodes of size 10 μm, 100 μm, and 0.5 mm. A one-electron oxidation wave was observed for the oxidation of nitrite, followed by a second (and sometimes third) oxidation peak at more positive potentials. The peak positions were observed at +0.2, +1.13, and + 1.57 V vs ferrocene (Fc, standard internal reference redox couple). These peaks were assigned to the oxidations of NO_2 and nitrate (NO_3^-), respectively. From chronoamperometry, a solubility value of 7.5 mM and a diffusion coefficient of 2.0×10^{-11} m^2 s^{-1} for KNO_2 were calculated. The oxidation of NO_2 gas was then studied. The gas is thought to be in equilibrium with its dimer, N_2O_4 in this medium. Two oxidative waves (+1.10 and +2.24 V vs Fc at 100 mV s^{-1} on the 100 μm diameter electrode) were observed, and are assigned to (a) the oxidation of N_2O_4 following a CE process given in eqs 9 and 10 and (b) the *direct* oxidation of N_2O_4 following an ECE process given in eqs 13, 14, and 10. An electrochemically irreversible reductive wave (at −0.31 V vs Fc) was also observed, although its identity is unknown. A diffusion coefficient of 1.6×10^{-10} m^2 s^{-1} and a solubility of ca. 51 mM were calculated, suggesting the possibility for using RTILs as potential media for the analytical sensing of NO_2 gas.

Acknowledgment. D.S.S. thanks Schlumberger Cambridge Research and L.A. thanks the Department of Education and Learning in Northern Ireland and Merck GmBH for financial support.

Supporting Information Available: Cyclic voltammograms for the oxidation of nitrite with an extended anodic window. This material is available free of charge via the Internet at http://pubs.acs.org.

References and Notes

(1) Alonso, A.; Etxaniz, B.; Martinez, M. D. *Food Addit. Contam.* **1992**, *9*, 111.
(2) Sanyal, S. *Bull. Electrochem.* **1990**, *6*, 392.
(3) Genders, J. D.; Hartsough, D.; Hobbs, D. T. *J. Appl. Electrochem.* **1996**, *26*, 1.
(4) Davis, J.; Moorcroft, M. J.; Wilkins, S. J.; Compton, R. G.; Cardosi, M. F. *Analyst* **2000**, *125*, 737.
(5) Moorcroft, M. J.; Davis, J.; Compton, R. G. *Talanta* **2001**, *54*, 785.
(6) Zhao, G.; Liu, K.; Lin, S.; Liang, J.; Guo, X.; Zhang, Z. *Microchim. Acta* **2004**, *144*, 75.
(7) Martins, M. E.; Calandra, A. J.; Arvía, A. J. *Electrochim. Acta* **1970**, *15*, 111.
(8) Calandra, A. J.; Arvía, A. J. *Electrochim. Acta* **1966**, *11*, 1173.
(9) Swofford, H. S., Jr.; McCormick, P. G. *Anal. Chem.* **1965**, *37*, 970.
(10) Topol, L. E.; Osteryoung, R. A.; Christie, J. H. *J. Phys. Chem.* **1966**, *70*, 2857.
(11) McCormick, P. G.; Swofford, H. S., Jr. *Anal. Chem.* **1969**, *41*, 146.
(12) Wargon, J. A.; Arvía, A. J. *Electrochim. Acta* **1971**, *16*, 1619.
(13) Wargon, J. A.; Arvía, A. J. *Electrochim. Acta* **1972**, *17*, 649.
(14) Caro, C. A.; Bedioui, F.; Zagal, J. H. *Electrochim. Acta* **2002**, *47*, 1489.
(15) Piela, B.; Wrona, P. K. *J. Electrochem. Soc.* **2002**, *149*, E55.
(16) Tanaka, N.; Kato, K. *Bull. Chem. Soc. Jpn.* **1956**, *29*, 837.
(17) Hoheráková, Z.; Opekar, F. *Sens. Actustors, B* **2004**, *97*, 379.
(18) Mizutani, Y.; Matsuda, H.; Ishiji, T.; Furuya, N.; Takahashi, K. *Sens. Actuators, B* **2005**, *108*, 815.
(19) Boughriet, A.; Wartel, M.; Fischer, J. C. *J. Electroanal. Chem.* **1985**, *190*, 103.
(20) Boughriet, A.; Wartel, M.; Fischer, J. C. *Talanta* **1986**, *33*, 385.
(21) Lee, K. Y.; Amatore, C.; Kochi, J. K. *J. Phys. Chem.* **1991**, *95*, 1285.
(22) Buzzeo, M. C.; Hardacre, C.; Compton, R. G. *Anal. Chem.* **2004**, *76*, 4583.
(23) Howlett, P. C.; MacFarlane, D. R.; Hollenkamp, A. F. *Electrochem. Solid State Lett.* **2004**, *7*, A97.
(24) McEwen, A. B.; Ngo, H. L. K. L.; Goldman, J. L. *J. Electrochem. Soc.* **1999**, *146*, 1687.
(25) Wang, P.; Zakeeruddin, S. M.; Moser, J. E.; Grätzel, M. *J. Phys. Chem. B* **2003**, *107*, 13280.
(26) Broder, T. L.; Silvester, D. S.; Aldous, L.; Hardacre, C.; Crossley, A.; Compton, R. G. *New J. Chem.* **2007**, DOI: 10.1039/b701097d.

(27) Bonhôte, P.; Dias, A. P.; Papageorgiou, N.; Kalyanasundaram, K.; Grätzel, M. *Inorg. Chem.* **1996**, *35*, 1168.
(28) Silvester, D. S.; Wain, A. J.; Aldous, L.; Hardacre, C.; Compton, R. G. *J. Electroanal. Chem.* **2006**, *596*, 131.
(29) Schröder, U.; Wadhawan, J. D.; Compton, R. G.; Marken, F.; Suarez, P. A. Z.; Consorti, C. S.; de Souza, R. F.; Dupont, J. *New J. Chem.* **2000**, *24*, 1009.
(30) Silvester, D. S.; Aldous, L.; Lagunas, M. C.; Hardacre, C.; Compton, R. G. *J. Phys. Chem. B* **2006**, *110*, 22035.
(31) Sharp, M. *Electrochim. Acta* **1983**, *28*, 301.
(32) Shoup, D.; Szabo, A. *J. Electroanal. Chem.* **1982**, *140*, 237.
(33) Evans, R. G.; Klymenko, O. V.; Saddoughi, S. A.; Hardacre, C.; Compton, R. G. *J. Phys. Chem. B* **2004**, *108*, 7878.
(34) Buzzeo, M. C.; Evans, R. G.; Compton, R. G. *ChemPhysChem* **2004**, *5*, 1106.
(35) Desimoni, E.; Palmisano, F.; Zambonin, P. G. *J. Electroanal. Chem.* **1977**, *84*, 315.
(36) Daniel, V.; Albright, J. G. *J. Chem. Eng. Data* **1995**, *40*, 519.
(37) Grützner, G.; Kuta, J. *Pure Appl. Chem.* **1984**, *56*, 461.
(38) Hultgren, V. M.; Mariotti, A. W. A.; Bond, A. M.; Wedd, A. G. *Anal. Chem.* **2002**, *74*, 3151.
(39) Rudolph, M.; Reddy, D. P.; Feldberg, S. W. *Anal. Chem.* **1994**, *66*, 589A.
(40) Buzzeo, M. C.; Klymenko, O. V.; Wadhawan, J. D.; Hardacre, C.; Seddon, K. R. *J. Phys. Chem. A* **2003**, *107*, 8872.